

Characterization of Fabric Tensile Loading Curve in Nonlinear Region Related to Their Structure; Part I: Woven Fabric

Kianoush Hosseini, Abdolhossein Sadeghi and Ali Asghar Asgharian Jeddi

Abstract—This study focuses on the tensile modulus and Poisson's ratio variations of woven fabric in nonlinear region of load-extension curve. This region of the curve can play as a control approach on the secondary modulus/primary modulus ratio. For this purpose, the fabric modulus and Poisson's ratio were determined for three different weave structures (plain, 1/3 twill, and 1/7 twill) in the warp and weft directions. The experimental results were analysed statistically to obtain the primary and secondary linear regions and also the nonlinear region of fabrics moduli. The analysis explain that the geometry of fabric structures such as the float and diagonal parts of yarn and also the yarn crimp in both warp and weft yarns have important role on the modulus and Poisson's ratio of fabrics in the nonlinear region. It was found that the greatest range of the nonlinear region in the warp direction is for plain then, 1/3 and 1/7 twill weaves, respectively, by reason of the increase of diagonal part of yarn and the decrease of float part of yarn in fabric structures, simultaneously. But, due to the buckling of the float part of yarn in the weft direction, the 1/7 twill weave has the greatest range of the nonlinear region and the plain weave has the least one.

Key words: Woven fabric, tensile modulus, Poisson's ratio, uniaxial tensile loading, nonlinear region.

I. INTRODUCTION

AS the woven fabric is subjected to uniaxial tensile loading at low levels, crimp interchange occurs as crimp of the yarns decreases in the loaded direction and increases in the cross direction. As the load is increased past the crimp interchange region, yarns in the loading direction are further extended. In this region of deformation, the main factor of further fabric deformation is due to yarn extension. The tensile behavior of woven fabric under a gradually increasing applied force is usually shown by the load-extension curve in which the slope of the primary linear region of the curve, low resistance region, is called as the primary modulus and the slope of the secondary linear region of the curve, high resistance region, is called as the secondary modulus [1-5]. There is a nonlinear region between these two linear regions that could be affected by the fabric structure (Figure 1). This nonlinear region can play very important role in the tensile

extension behavior of fabric. For instance, we need sometimes to have a very easy extension of fabric at the start of loading and at the end a severe extension (e.g.: ventricular restraint device, protection nets, and composite fabrics in molding process). In this case, the range of nonlinear region should be very short.

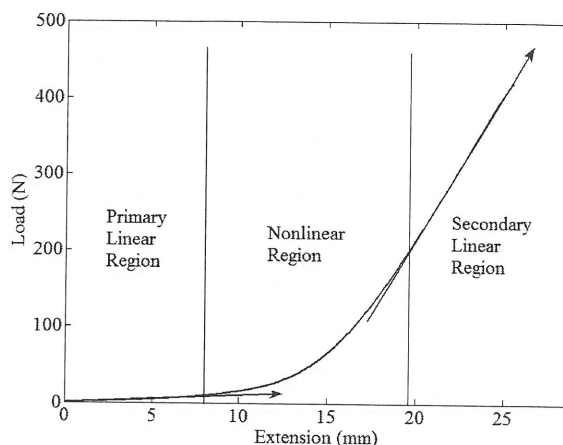


Fig. 1. Load-extension curve of woven fabric.

The pioneer in the investigation of tensile deformation of woven fabrics is Peirce [6]. He began this investigation from the viewpoint of the geometrical analysis of the weave. Grosberg and Kedia [7] analysed the initial load-extension modulus of a cloth and showed that it depends not only on the bending modulus of the yarn and the geometry it takes up in the cloth, but also on the strain history of the fabric. Kawabata, Niwa, and Kawai [8-9] presented the uniaxial and biaxial tensile deformation theories for plain woven fabrics based on their structural mechanics. Both the uniaxial and biaxial tensile properties were successfully calculated with the aid of these models. Realff [3] in study on the plain weave fabric expressed as the amount of yarn crimp increases, the extent of the crimp interchange region increases and thus, fabric breaking extension increases. She found that with the change of weave density, the amount of yarn crimp changes. In continuation, Realff, Boyce, and Backer [4] introduced a micromechanical model in which the entire uniaxial tensile stress-strain behavior of the woven fabric is modeled from the constitutive yarn properties and the original fabric geometry. To predict the behavior of woven fabric in uniaxial tension and relaxation, Halleb and Amar [10] proposed a rheological model with 15 coefficients that are

K. Hosseini, A. Sadeghi and A. A. A. Jeddi are with the Department of Textile Engineering of Amirkabir University of Technology, Tehran, Iran. Correspondence should be addressed to A. A. A. Jeddi (e-mail: ajeddi@aut.ac.ir).

identified from the tests. An artificial neuronal network trained with a retro-propagation algorithm performs functional mapping between these mechanical coefficients and the technical parameters of fabric, which allows predicting the mechanical behavior of fabrics starting only from their technical parameters. In continuation of their study, Halleb & Amar [11] modified the rheological model and proposed an analytical model with 10 coefficients in order to simplify the procedure of identification and to diminish the experimental work. Somodi *et al.* [12] presented a micromechanical model of the tensile behavior of woven fabric in which the model covers both geometric and material nonlinearities in fabric deformation with a limited set of basic parameters. In order to refine the initial estimate, these set of parameters were optimized using genetic algorithm. The results obtained of the model showed good agreement with the experimental ones.

Leaf and Kandil [13] introduced a straight-line or saw-tooth model to represent an idealized woven fabric and presented an analysis of the initial load-extension behavior of plain woven fabrics. A closed-form analytical solution

II. MATERIALS AND METHODS

Woven fabrics with different weave structures including plain, 1/3, and 1/7 twill weaves were produced using 153 denier (17 tex) polyester filament for warp yarn and 16.63 Ne (35.5 tex) ring-spun cotton for weft yarn. These fabrics were woven on a dobby weaving machine with weave width of 155 cm, and the same warp and weft weave densities. Then, they were finished under normal industrial conditions as follows. All woven fabrics were first washed in an air jet machine with a solution of 0.5 g/lit detergent at boiled temperature. Washed fabrics were then dried with a hot steam of 120 °C.

The tensile properties of fabrics were obtained according to the standard ISO 13934-1:1999 using a CRE tensile tester with a crosshead speed of 100 mm/min and a gauge length of 200 mm. Other properties of fabrics such as crimp, weave density, mass per unit area, and thickness were measured according to the standards ASTM D 3883-04, D 3775-08, D 3776-09, and D 1777-96. The values of these physical and mechanical properties are given in

TABLE I
PHYSICAL AND MECHANICAL PROPERTIES OF TESTED WOVEN FABRICS

Weave structure	Weave density [cm ⁻¹]		Crimp [%]		Breaking force		Breaking extension		Mass per unit area [g/m ²]	Thickness [mm]
	Warp	Weft	Warp	Weft	[N]		[mm]			
					Warp	Weft	Warp	Weft		
Plain	41	20.8	9	6	1245	449	78	15.15	154	0.35
1/3 Twill	42.3	20.95	7	9	1287	428	68	22	158	0.44
1/7 Twill	44.3	21.2	5.5	11.5	1295	411	57.5	28.2	163	0.63

was found for the initial Young's modulus and the Poisson's ratio of the fabric, when the yarns were assumed to be inextensible and incompressible. Bais-Singh *et al.* [14] presented an experimental method based on video recording and image analysis to characterize the lateral contraction of nonwoven fabrics during uniaxial tensile deformation. They indicated that the Poisson's ratio can also be readily estimated using this method. Sun *et al.* [15] developed a mechanical model for a woven fabric made of extensible yarns to calculate the fabric Poisson's ratios. They showed that the Poisson's ratio in a woven fabric arises from the interaction between the warp and weft yarns, and can be expressed in terms of the structural and mechanical parameters of the system. Hursa *et al.* [16] presented a digital image correlation method for the determination of Poisson's ratio of woven fabric and indicated that the value of the Poisson's ratio depends on the weave type and the number of yarns in the fabric.

The present paper investigates the tensile modulus and Poisson's ratio variations of the woven fabric in nonlinear region of load-extension curve. In this investigation, it is attempted to analyze these parameters based on the variations of the warp and weft yarn crimps and woven fabric structures.

Table I.

A. Determination of nonlinear region of load-extension curve

To measure the tensile properties of the woven fabrics from each weave structure five specimens were tested in the warp and weft directions. The data of the load and extension were recorded at extension intervals of 0.0833 mm by the tensile tester. Then, the load-extension curves of the fabrics were plotted using these data. To determine the fabric moduli values in different regions of the curve, the slopes of load-extension curve are obtained at the points with extension intervals of 1 mm (twelve times of interval between two successive recorded data i.e. 12×0.0833 mm = 1 mm) from zero to the breaking extension. These slopes were calculated by written a program in MATLAB and using the nine-point central difference with the following equation [17]. (The nine point central difference method is more accurate than the calculation "y" using only one point.):

$$f'_x = \frac{1}{840h} (3f_{x-4h} - 32f_{x-3h} + 168f_{x-2h} - 672f_{x-h} + 672f_{x+h} - 168f_{x+2h} + 32f_{x+3h} - 3f_{x+4h}) \quad (1)$$

TABLE II
RESULTS OF HOMOGENEOUS SUBSETS RELATED TO TUKEY TEST FOR THE 1/7 TWILL WEAVE IN THE WEFT DIRECTION

Extension (mm)	N	Subset for alpha = 0.05														
		1	2	3	4	5	6	7	8	9	10	11	12	13	14	15
1	5	0.2														
2	5	0.2														
4	5	0.5														
3	5	0.7														
5	5	0.8														
6	5	1.2	1.2													
9	5	1.3	1.3													
7	5	1.4	1.4	1.4												
8	5	1.5	1.5	1.5												
10	5		2.6	2.6	2.6											
11	5			3.0	3.0											
12	5				3.7											
13	5					6.1										
14	5					7.4										
15	5						10.2									
16	5							12.7								
17	5								16.0							
18	5									20.4						
19	5										24.0					
20	5											26.2				
21	5												29.2			
22	5													31.8		
23	5														34.0	
24	5														35.5	35.5
25	5															36.6
27	5															36.7
28	5															36.7
26	5															37.2
Sig.		0.28	0.37	0.05	0.66	0.40	1.00	1.00	1.00	1.00	1.00	1.00	1.00	1.00	0.11	0.05

where f'_x is the value of slope (modulus) at x mm extension. Also, $h = 0.0833$ mm is interval between two successive recorded data and f_{x+h} , f_{x+2h} , f_{x+3h} , f_{x+4h} , f_{x-h} , f_{x-2h} , f_{x-3h} and f_{x-4h} are the values of load at $x+h$, $x+2h$, $x+3h$, $x+4h$, $x-h$, $x-2h$, $x-3h$, $x-4h$ mm extension, respectively. These calculations were performed for all the plotted load-extension curves of each weave structure in both warp and weft directions. The data of slopes of each interval were analysed for significance in differences, using one-way ANOVA test at the 95% level of confidence. Therefore, Tukey test was performed to categorize the homogeneous subsets. As a typical calculation, these homogeneous subsets are displayed in Table II for the 1/7 twill weave structure in the weft direction. The first and last subsets are contained the lowest and highest values, respectively. The first subset (the slopes values at nine first points) indicates the primary linear region of the load-extension curve as the primary modulus of fabric, while the last subset (the slopes values at five last points) indicates the secondary linear region of the curve as the secondary modulus. Therefore, the nonlinear region of the load-extension curve between these two linear regions is determined as the nonlinear region of the fabric modulus.

B. Determination of Poisson's ratio

To determine Poisson's ratio, the fabric specimens were prepared according to the standard of the tensile properties. A black ring with internal diameter of 25 mm was drawn by stamping method in the center of the fabric specimens to avoid the jaw and edge effects during measurement. The fabric specimens prepared in this way were placed on the tensile tester and illuminated by halogen bulb lamp. When the fabric specimen is subjected to uniaxial tensile loading, the black ring is deformed from circular to elliptical shape and hence, the sizes of the horizontal and vertical diameters are changed. This process was recorded by a digital video camera Canon MV750i which was placed on a tripod in front of the tensile tester, as by the experimental scheme shown in Figure 2. The digital video camera had a resolution of 720×576 pixels², could capture 25 frames per second and was connected to a computer through a video capture card. This interface device was used for recording from the digital video camera to the computer. In this way, the video recording was saved on a computer hard disk drive in AVI format. It should be mentioned that the digital video camera started to record moments before the fabric specimen is subjected to uniaxial tensile loading. Hence, using the Ulead VideoStudio software, a part of the

video recording which is belonged to the jaw stationary position of the tensile tester was removed. The edited video recording in AVI format was loaded into the VirtualDub program in which every frame was extracted as an image in BMP format. Then, the Poisson's ratio is measured at extension intervals of 1 mm. With regards to the framing rate of the digital video camera (25 fps) and the crosshead speed of tensile tester (100 mm/min), the images with intervals of 15 frames which correspond to these levels of extension were chosen.

It should be mentioned that the distance between two points from an image could be expressed based on the number of pixels between them. Hence, using Adobe Photoshop software, the number of pixels of the internal horizontal and vertical diameters of the ring was obtained from the first image. Afterward, the number of pixels of the deformed rings diameters was obtained from the next corresponding images. Then, the strains in the horizontal direction (ϵ_{x_i}) and vertical direction (ϵ_{y_i}) at the various levels of extension were calculated according to the Eqs (2) and (3).

$$\epsilon_{x_i} = \frac{x_{d_i} - x_r}{x_r} \quad (2)$$

$$\epsilon_{y_i} = \frac{y_{d_i} - y_r}{y_r} \quad (3)$$

where x_{d_i} and y_{d_i} are the number of pixels of the internal horizontal and vertical diameters of the deformed rings at the various levels of extension (i = the number of start point to the end of nonlinear region of fabric modulus in load-extension curve), respectively, and x_r and y_r are the number of pixels of the same diameters of the ring before extension. After finding the values of ϵ_{x_i} and ϵ_{y_i} , the Poisson's ratio values (ν_i) at the various levels of extension were finally calculated using Eq. (4).

$$\nu_i = -\frac{\epsilon_{x_i}}{\epsilon_{y_i}} \quad (4)$$

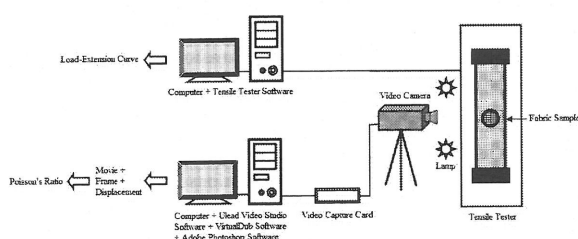


Fig. 2. Experimental scheme.

III. RESULTS AND DISCUSSION

The average load-extension curves of the fabrics with weave structures plain, 1/3 and 1/7 twill in the warp and weft directions are shown in Figure 3 (a) and b, respectively.

The range of the nonlinear region of the load-extension curves was determined corresponding to the Methods section (Table III). Also, the moduli values in this region

are given at the intervals of 1 mm in Table IV.

The Poisson's ratios of the fabrics were also calculated in the same nonlinear region of the load-extension curves at the intervals of 1 mm (Table V).

A. Warp direction characterization

With regard to Figure 4, it is observed that in the warp direction, the greatest range of the nonlinear region is belonged to the plain then, 1/3 and 1/7 twill weaves, respectively. Whereas, the plain weave has the least rate of modulus variations in the nonlinear region then, 1/3 and 1/7 twills, respectively. These behaviors can be attributed to the amount of yarn crimp in this direction. As it is shown in Figure 4, by increasing the amount of yarn crimp in fabric structures, the range of the nonlinear region increases and the rate of modulus variations in this region decreases.

In the same range of nonlinear region, Figure 5 shows the greatest rate of Poisson's ratio variations is related to the 1/7 twill then, 1/3 twill and plain weaves, respectively. In other words, by increasing the amount of yarn crimp, the rate of Poisson's ratio variations decreases.

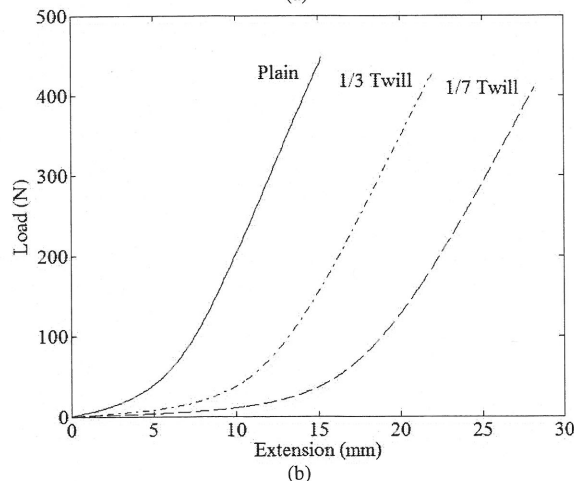
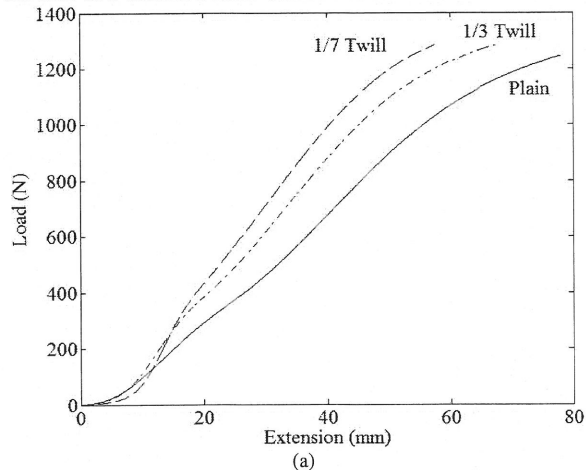


Fig. 3. Load-extension curves of woven fabrics for different weave structures: (a) warp direction (b) weft direction.

It should be mentioned that the amount of yarn crimp could be affected by the structural parameters of woven fabric such as the diagonal and float parts of yarn, as

shown in Figure 6. The number of these parameters is given for the equal weave width (four repeat of plain weave, two repeat of 1/3 twill weave, and one repeat of 1/7 twill weave) in Table VI. It can be concluded that with the increase of the number of diagonal part of yarn in fabric structure, the amount of yarn crimp in the warp direction increases. Also, with the increase of the number of float part of yarn, the amount of yarn crimp in this direction decreases.

TABLE III
RANGE OF NONLINEAR REGION OF THE LOAD-EXTENSION CURVES OF FABRICS FOR DIFFERENT WEAVE STRUCTURES

Weave structure	Plain		1/3 Twill		1/7 Twill	
	Warp	Weft	Warp	Weft	Warp	Weft
Range of nonlinear region (mm)	3-33	3-10	3-29	5-17	5-23	10-23

TABLE IV
MODULI VALUES IN NONLINEAR REGION OF THE LOAD-EXTENSION CURVES OF FABRICS FOR DIFFERENT WEAVE STRUCTURES

Range of extension in nonlinear region (mm)	Modulus value (N/mm)					
	Plain		1/3 Twill		1/7 Twill	
	Warp	Weft	Warp	Weft	Warp	Weft
3	5.10	8.07	4.36			
4	6.99	10.90	6.21			
5	9.54	16.04	9.31	3.14	4.17	
6	11.53	21.84	12.04	3.10	5.89	
7	14.48	30.09	16.69	4.16	8.88	
8	16.30	37.44	20.04	5.96	13.67	
9	17.85	42.03	24.52	8.73	19.72	
10	18.83	45.32	28.06	12.25	27.88	2.61
11	19.88		31.37	16.33	34.88	3.08
12	20.20		32.23	21.52	41.29	3.76
13	20.49		33.06	26.55	44.42	6.14
14	20.36		31.12	30.58	44.16	7.44
15	20.11		28.40	33.79	41.27	10.29
16	20.39		26.46	36.44	37.45	12.73
17	19.32		23.88	38.09	33.32	16.07
18	18.40		21.39		29.14	20.49
19	18.11		20.12		27.11	24.02
20	17.13		19.22		25.89	26.22
21	16.35		19.94		25.72	29.29
22	16.51		20.12		26.22	31.85
23	15.79		21.03		27.11	34.03
24	16.21		22.71			
25	17.22		23.08			
26	17.02		24.44			
27	17.33		25.14			
28	18.18		25.82			
29	18.75		25.52			
30	18.80					
31	19.91					
32	20.10					
33	20.57					

TABLE V
POISSON'S RATIOS VALUES IN NONLINEAR REGION OF THE LOAD-EXTENSION CURVES OF FABRICS FOR DIFFERENT WEAVE STRUCTURES

Range of extension in nonlinear region (mm)	Poisson's ratio value					
	Plain		1/3 Twill		1/7 Twill	
	Warp	Weft	Warp	Weft	Warp	Weft
3	0.095	0.254	0.221			
4	0.117	0.360	0.260			
5	0.154	0.425	0.314	0.326	0.276	
6	0.187	0.460	0.361	0.343	0.341	
7	0.228	0.487	0.400	0.360	0.435	
8	0.280	0.510	0.474	0.390	0.524	
9	0.323	0.498	0.532	0.398	0.619	
10	0.350	0.481	0.588	0.422	0.714	0.237
11	0.378		0.638	0.429	0.779	0.248
12	0.402		0.696	0.435	0.833	0.254
13	0.434		0.744	0.448	0.861	0.271
14	0.472		0.779	0.436	0.857	0.279
15	0.496		0.801	0.421	0.841	0.289
16	0.521		0.810	0.404	0.815	0.298
17	0.540		0.798	0.382	0.787	0.308
18	0.559		0.780		0.756	0.315
19	0.569		0.764		0.724	0.310
20	0.578		0.745		0.695	0.303
21	0.582		0.723		0.669	0.291
22	0.572		0.705		0.645	0.279
23	0.567		0.689		0.623	0.267
24	0.560		0.672			
25	0.549		0.656			
26	0.541		0.637			
27	0.535		0.618			
28	0.530		0.596			
29	0.523		0.579			
30	0.514					
31	0.506					
32	0.498					
33	0.490					

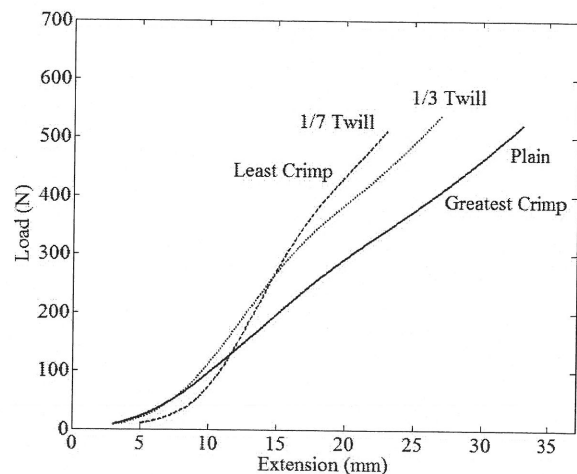


Fig. 4. Nonlinear region of the load-extension curves of fabrics for different weave structures in the warp direction.

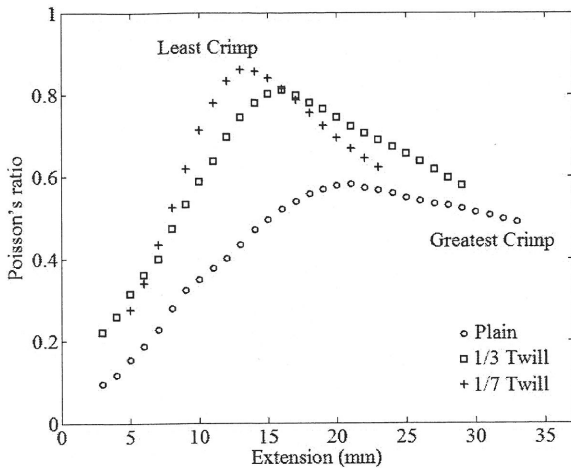


Fig. 5. Poisson's ratio of fabrics for different weave structures in nonlinear region of load-extension curves in the warp direction.

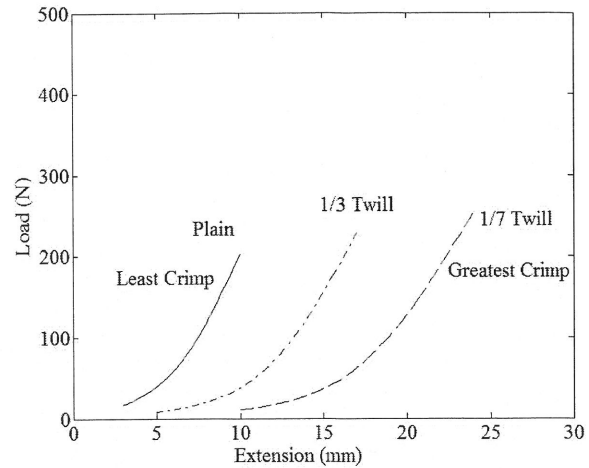


Fig. 7. Nonlinear region of the load-extension curves of fabrics for different weave structures in the weft direction.

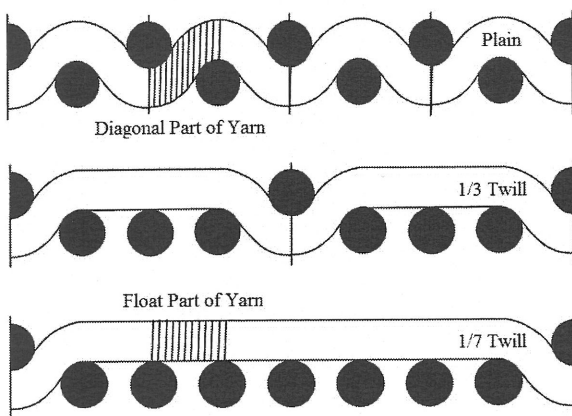


Fig. 6. Structural parameters of woven fabric: diagonal and float parts of yarn.

TABLE VI. NUMBER OF STRUCTURAL PARAMETERS IN THE EQUAL WIDTH, CRIMP, AND WIDTH SHRINKAGE FOR PLAIN, 1/3 AND 1/7 TWILL WEAVES

Weave structure	Diagonal part of yarn	Float part of yarn	Fabric width shrinkage [%]	Crimp [%]	
				Warp	Weft
Plain	(4)×2	-	0.12	9	6
1/3 Twill	(2)×2	(2)×2	3.03	7	9
1/7 Twill	(1)×2	(1)×6	7.41	5.5	11.5

B. Weft direction characterization

With regard to Figure 7, it is observed that in the weft direction, the greatest range of the nonlinear region is belonged to the 1/7 twill then, 1/3 twill and plain weaves, respectively. Whereas, the rate of modulus variations in this region are increased from 1/7 twill to 1/3 twill and plain weaves, respectively. These behaviors in the weft direction are reversed to the warp direction with similar explanation of yarn crimp. It means that, by increasing the amount of yarn crimp, the range of the nonlinear region increases whereas, the rate of modulus variations decreases. Considering Figure 8, it is observed that by increasing the amount of yarn crimp, the rate of Poisson's ratio variations decreases.

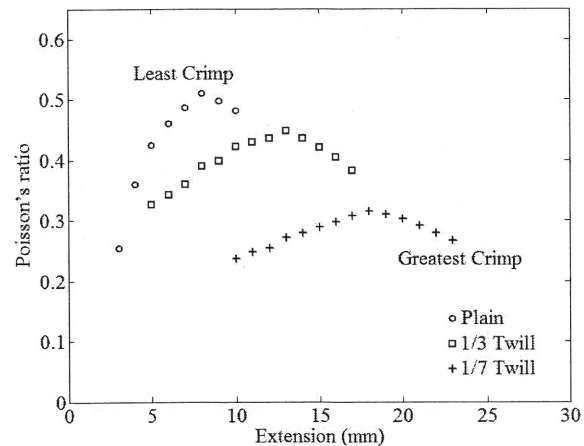


Fig. 8. Poisson's ratio of fabrics for different weave structures in nonlinear region of load-extension curves in the weft direction.

To account for the mentioned analysis for the nonlinear extension behavior of fabrics in more detail based on their structures, the following explanation is presented. Table VI shows that the width shrinkage of plain weave after temple and finishing treatment is negligible, while for 1/3 and 1/7 twill weaves are considerable. The cause of this decrease can be attributed to the existence of the float part of yarn in these two weaves. With the increase of the number of float part of yarn, the amount of decrease of fabric width increases. During the width decreasing, the buckling of the float part of weft yarn is occurred (Figure 9). Consequently, the amount of yarn crimp in the weft direction increases. As it has been given in Table VI, in opposite to the warp direction, the 1/7 twill weave has the greatest amount of yarn crimp and the plain weave has the least amount in the weft direction.

As it has been given in Table I, the weft yarn density in opposite to the warp yarn density is nearly constant that it means the change of fabrics length is negligible. The reason of this phenomenon is during weaving process that the fabric is gripped in the warp direction by the warp beam and the cloth roller. Since the fabric width decreases after the temple, thus the warp yarns are locked by the weft

yarns. Hence, there is no possibility for fabric length to be decreased as demonstrated in Figure 10.

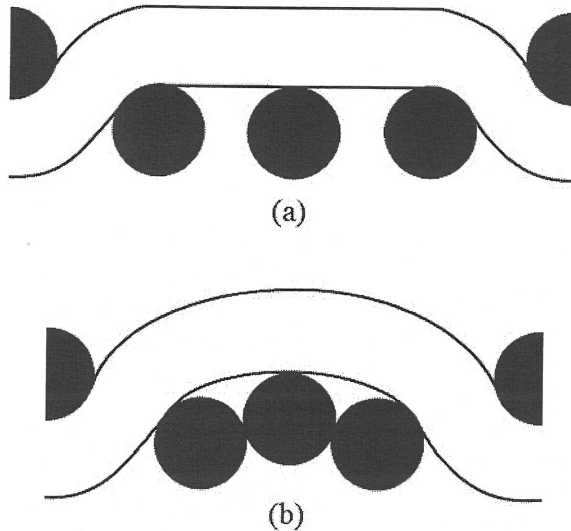


Fig. 9. The increase of warp yarn density (black) and the buckling of float part of weft yarn (white) during decrease of fabric width: (a) before buckling (b) after buckling.

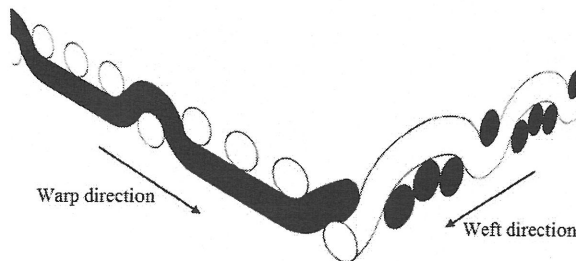


Fig. 10. To lock the warp yarns by the weft yarns.

IV. CONCLUSIONS

The nonlinear region of load-extension curve of woven fabric is considered as an important role in the tensile extension behavior of fabric. In this study, it was found that the geometry of fabric structures has a considerable influence on the tensile modulus and Poisson's ratio variations of woven fabric. The following points are also concluded from this investigation:

In the warp direction, the greatest range of the nonlinear region is for plain then, 1/3 and 1/7 twill weaves, respectively. This trend is reverse for the rate of tensile modulus variations and the rate of Poisson's ratio variations in the same region.

With the increase of diagonal part of yarn in fabric structure, the range of the nonlinear region is increased. With the increase of float part of yarn in fabric structure, the range of the nonlinear region is decreased.

In the weft direction, the greatest range of the nonlinear region is for the 1/7 twill then, 1/3 twill and plain weaves, respectively. It was attributed to the buckling of the float part of yarn in weft direction.

REFERENCES

- [1] T. B. Langston, "The Mechanical behavior of air textured aramid yarns in thermoset composites", M. S. thesis, Dept. Text. Eng., NCS University, Raleigh, N.C., 2003.
- [2] W. E. Morton and J. W. S. Hearle, *Physical Properties of Textile Fibers*. Cambridge: Woodhead Publishing Limited, 2008.
- [3] M. L. Realff, "Identifying local deformation phenomena during woven fabric uniaxial tensile loading", *Text. Res. J.* vol. 64, no. 3, pp. 135–141, 1994.
- [4] M. L. Realff, M. C. Boyce and S. Backer, "A micromechanical model of the tensile behavior of woven fabric", *Text. Res. J.*, vol. 67, no. 6, pp. 445–459, 1997.
- [5] B. P. Saville, *Physical Testing of Textiles*. Cambridge: Woodhead Publishing Limited, 1999.
- [6] F. T. Peirce, "The geometry of cloth structure", *J. Text. I.*, vol. 28, pp. 45–96, 1937.
- [7] P. Grosberg and S. Kedia, "The mechanical properties of woven fabrics. Part I: The initial load-extension modulus of woven fabrics", *Text. Res. J.*, vol. 36, No. 1, pp. 71–79, 1966.
- [8] S. Kawabata, M. Niwa and H. Kawai, "The finite deformation theory of plain weave fabrics. Part I: The biaxial deformation theory", *J. Text. I.*, vol. 64, No. 1, pp. 21–46, 1973.
- [9] S. Kawabata, M. Niwa and H. Kawai, "The finite deformation theory of plain weave fabrics. Part II: The uniaxial deformation theory", *J. Text. I.*, vol. 64, no. 2, pp. 47–61, 1973.
- [10] N. Halleb and S. B. Amar, "Prediction of fabrics mechanical behaviour in uni-axial tension starting from their technical parameters", *J. Text. I.*, vol. 99, no. 6, pp. 525–532, 2008.
- [11] N. Halleb and S. B. Amar, "Model modification and prediction of mechanical behavior of fabrics in uniaxial tension", *J. Text. I.*, vol. 101, no. 8, pp. 707–715, 2010.
- [12] Z. Somodi, T. Rolich, A. Hursa and D. Z. Pavlinic, "Micromechanical tensile model of woven fabric and parameter optimization for fit with KES data", *Text. Res. J.*, vol. 80, no. 13, pp. 1255–1264, 2010.
- [13] G. A. V. Leaf and K. H. Kandil, "The initial load-extension behavior of plain woven fabrics", *J. Text. I.*, vol. 71, no. 1, pp. 1–7, 1980.
- [14] S. Bais-Singh, R. D. Anandjiwala and B. C. Goswami, "Characterizing lateral contraction behavior of spunbonded nonwovens during uniaxial tensile deformation", *Text. Res. J.*, vol. 66, no. 3, pp. 131–140, 1996.
- [15] H. Sun, N. Pan and R. Postle, "On the Poisson's ratios of a woven fabric", *Composite Structures*, vol. 68, no. 4, pp. 505–510, 2005.
- [16] A. Hursa, T. Rolich and S. E. Razic, "Determining pseudo Poisson's ratio of woven fabric with a digital image correlation method", *Text. Res. J.*, vol. 79, no. 17, pp. 1588–1598, 2009.
- [17] F. B. Hildebrand, *Introduction to Numerical Analysis*. New York: Dover Publications, 1987.